

## บทความวิจัย

# ฟังก์ชันการกระจายแบบคู่และปัจจัยโครงสร้างของโลหะไฮโดรเจนเหลวจากแบบจำลองทรงกลมแข็งชนิดที่ขึ้นกับอุณหภูมิศาสตร์

วิชิต ศรีตระกูล<sup>1\*</sup> และ รังสรรค์ โกญจนานุกรม<sup>2</sup>

### บทคัดย่อ

งานวิจัยนี้ได้คำนวณฟังก์ชันการกระจายแบบคู่และปัจจัยโครงสร้างของโลหะไฮโดรเจนเหลวที่ความหนาแน่น และความดันต่างๆ กันหลายค่า โดยใช้สมการออร์บิทัลและเซอร์นิกกับแบบจำลองทรงกลมแข็งชนิดที่ขึ้นกับอุณหภูมิศาสตร์ และใช้การประมาณของเปอร์คัส-เยวิกเพื่อที่จะหาผลลัพธ์ของฟังก์ชันการกระจายแบบคู่พร้อมกับปัจจัยโครงสร้างโดยใช้รัศมีของทรงกลมแข็งต่างกันสามค่า หลังจากนั้นจึงใช้ปริมาณเหล่านี้ไปหาสภาพนำไฟฟ้าโดยใช้สูตรของไซแมนที่รู้จักกันดี ผลที่ได้สรุปว่า การเปลี่ยนสถานะระหว่างโลหะกับฉนวนของโลหะไฮโดรเจนเหลวเกิดจากความดันที่เพิ่มขึ้น และคาดว่าเกิดขึ้นเมื่อปัจจัยโครงสร้างมีขนาดพาดผ่านค่า  $2k_F$

**คำสำคัญ:** ฟังก์ชันการกระจายแบบคู่ ปัจจัยโครงสร้าง โลหะไฮโดรเจนเหลว แบบจำลองทรงกลมแข็ง สูตรของไซแมน

<sup>1</sup>ภาควิชาฟิสิกส์ คณะวิทยาศาสตร์ จุฬาลงกรณ์มหาวิทยาลัย

<sup>2</sup>สาขาวิชาวิทยาศาสตร์กายภาพ คณะวิทยาศาสตร์และเทคโนโลยี มหาวิทยาลัยหัวเฉียวเฉลิมพระเกียรติ

\*ผู้นิพนธ์ประสานงาน, e-mail: wichit.s@chula.ac.th

# Pair Distribution Function and Structure Factor of Liquid Metallic Hydrogen from Thermodynamic Dependent Hard Sphere Model

Wichit Sritrakool<sup>1\*</sup> and Rangsun Konjanatnikorn<sup>2</sup>

---

## ABSTRACT

The pair distribution function and structure factor of liquid metallic hydrogen at various densities and pressures are determined using the Ornstein-Zernike equation and the thermodynamic dependent hard-sphere model. The Percus-Yevick approximation is employed to solve for the pair distribution function at three different hard sphere radii. Consequently, the structure factor is determined from the pair distribution function and then employed to determine the electrical resistivity using the well known Ziman's formula. We conclude from the result that the metal-insulator transition of the metallic hydrogen due to pressure is speculated to occur if the first structure factor peak passes across  $2k_F$ .

**Keywords:** pair distribution function, structure factor, liquid metallic hydrogen, hard sphere model, Ziman's formula

---

<sup>1</sup>Department of Physics, Faculty of Science, Chulalongkorn University

<sup>2</sup>Department of Physics, Faculty of Science and Technology, Huachiew Chalermprakiet University

\*Corresponding author, e-mail: wichit.s@chula.ac.th

## Introduction

In 1996, Weir et al. [1] have reported their success in making liquid metallic hydrogen (LMH) under the high pressures between 93 to 180 GPa and high temperatures between 2,200 to 4,400 Kelvin. The densities of the liquid metallic hydrogen associated to these pressures and temperatures have been determined to be in the range of 0.28 to 0.36 moles per milliliter. The resistivity was found to decrease for four order of magnitudes, from  $10^6 \mu\Omega\text{-cm}$  to about  $500 \mu\Omega\text{-cm}$ . They expected that its conductivity decreases exponentially from a constant value  $\sigma_0$  like the Boltzmann factor, i.e.  $\sigma = \sigma_0 \exp[-E_g(d)/k_B T]$ , where  $E_g$  is the energy gap which is dependent on the density  $d$  of liquid metallic hydrogen. This experiment has confirmed the long-ago prediction of Wigner and Huntington [2] about the metal-insulator transition in pressurized hydrogen. Later in 2001, the same group of physicists [3] as in ref. [1] has also published similar results in liquid oxygen. The problem of LMH has been of interested till present days. In 2006 Shvets et al. [4] has determined the resistivity of metallic hydrogen by employing the perturbation theory in the electron-proton interaction. Thermodynamics of the proton subsystem is assumed to be given by the Percus-Yevick equation. The hard-sphere potential is used in the calculation. Shivets [5] has also determined the equation of state of liquid metallic hydrogen for the temperature range of 3,000 to 20,000 K and densities from 0.2 to 3 mole/cm<sup>3</sup>, which correspond to both experimental conditions on earth and in the cores of giant planets such as Jupiter and Saturn. In his calculation the hydrogen was assumed to be in atomic state and all its electrons were collectivized. Perturbation theory with the hard-sphere model was used in the electron-proton interaction. Recently, in 2008 Shivets [6] has determined the electrical conductivity of LMH at a temperature of 3,000 K and density of 0.3 mole/cm<sup>3</sup>. Hydrogen was treated as a ternary system. One subsystem was provided by protons and the second one-by neutral atoms of hydrogen. The third subsystem was the electron which was modeled by the nearly free electron. The simple hard-sphere model was used in this calculation.

It is therefore interesting for physicists to find out the mechanism of this transition and conditions to have this metallic state. To get these answers, one has to know the microscopic structure of liquid, especially the LMH being considered. There should not be long-range periodic structure in liquid since the constituent atoms or molecules are not localized. There are interactions between ions and ions, ions and electrons, and also electrons and electrons. The potential energy between ions and ions is the key interaction leading to a microscopic quantity of the system called pair distribution function (PDF). The PDF tells a chance (or probability) to find another particle at a distance measured from the center of a particle of interest.

Many authors have determined the transition pressure of hydrogen from insulator to metallic phase to be about 250 GPa. At room temperature and normal pressure on the earth surface ( $\sim 10^{-4}$  GPa), Hydrogen is in molecular form of gas. At huge pressure of about 100 GPa, hydrogen could not be in molecular form any more. Ceperley and Adler [7] have used the quantum theory with the diffusion Monte Carlo method to determine the transformation of hydrogen from molecular to atomic form at the pressure of about 300 GPa. Later, Barbee et al. [8] have used the local density approximation (LDA) to predict that hydrogen molecules will diminish at the pressure of about 380 GPa. In 1995, Holmes et al. [9] have proposed that hydrogen molecules partially transform to atomic form and therefore hydrogen is a mixture. The fraction of atomic hydrogen will increase as a function of pressure. For example, there is about 5% of atomic hydrogen at the pressure of 140 GPa and at 300 Kelvin. There is also another aspect of liquid metallic hydrogen seen by Kohanoff and Hansen [10]. They see metallic hydrogen as plasma at high pressures and high temperatures. Valence electrons behave like free fermions which do not attach to the core ions any more. Electrons therefore are treated as a rigid homogeneous Fermion gas with positive core ions suspending among them. This model is known as the one-component plasma (OCP), and is similar to the conventional model of normal metals. Ceperley [11] has used a numerical method called “path integral Monte Carlo” to determine the PDF.

In this paper, we use the hard sphere model and the pair correlation function derived by Wertheim [12,13] to determine the PDF of LMH. Instead of a constant value, we assume the hard sphere radius to be dependent on the thermodynamic quantities of the system such as density, temperature and pressure. Our calculated PDF's at various pressures are compared with the results of Xu and Hansen [15] who employed the density functional theory (DFT). Furthermore, we also determine from our PDF's the structure factor at corresponding pressures. Consequently, the structure factor is employed to determine the electrical resistivity using the well known Ziman's formula. The results are presented in the last section.

## Method

The system being considered is in a thermal equilibrium and consists of a very large number of atoms, say  $N$ , which approaches infinity. Let  $V$  be the volume which is also very large compared to the atomic volume. The PDF of an isotropic and homogeneous liquid is determined from the average counting number of atoms away at a point  $r$  from a particle of interest, namely

$$g(r) \equiv \frac{1}{Vd^2} \left\langle \sum_{i < j} \delta(\vec{r} - \vec{r}_{ij}) \right\rangle \quad (1)$$

where  $d$  is the number density or number of atoms per unit volume, i.e.  $N/V$ , which must be finite; and  $r_{ij}$  is the distance from atom  $i$  to atom  $j$ . Physically, the PDF tells us about the chance to find another particle next to the center of the interested particle. In case of an ideal atomic gas that has no correlation among the atomic constituents,  $g(r) = 1$ . For the liquid or other systems with correlation among atoms,  $g(r)$  oscillates around  $g(r) = 1$  and converges to unity at infinity. The distance from the origin to the first peak of  $g(r)$  tells us about the distance for the first chance to find another atom. The structure factor of a system defined as

$$S(k) \equiv \frac{1}{N} \left\langle \sum_{i \leq j} \exp(i\vec{k} \cdot \vec{r}) \right\rangle. \quad (2)$$

This quantity can be determined experimentally and theoretically can be written as a function of the PDF as

$$S(k) = 1 + d \int \exp(i\vec{k} \cdot \vec{r})(g(r) - 1) d\vec{r}. \quad (3)$$

The PDF can also be used to determine other physical quantities of the system such as the internal energy, the pressure, the compressibility, the chemical potential, etc.

Ornstein and Zernike were the very first persons who suggested about the correlation functions. They defined the total correlation function  $h(\vec{r}_{12})$  as a collection of correlation among particles in the system, where  $\vec{r}_{12}$  is the displacement of any two particles, namely

$$h(\vec{r}_{12}) = c(\vec{r}_{12}) + d \int_V c(\vec{r}_{13})c(\vec{r}_{23})d\vec{r}_3 + d^2 \int_V c(\vec{r}_{13})c(\vec{r}_{34})c(\vec{r}_{42})d\vec{r}_3d\vec{r}_4 + \dots \quad (4)$$

or

$$h(\vec{r}_{12}) = c(\vec{r}_{12}) + d \int_V c(\vec{r}_{13})h(\vec{r}_{23})d\vec{r}_3. \quad (5)$$

This equation is known as the Ornstein-Zernike (OZ) equation. Physically, the first part  $c(\vec{r}_{12})$  is called the pair correlation function and contributed from sole interaction between the first and the second particles while the integral term is contributed from other ambient particles. Hence, in the isotropic case the total correlation function will be

$$h(r) = c(r) + d \int_V c(r')h(|\vec{r} - \vec{r}'|)dr' \quad (6)$$

We may see that eq. (6) is a function of itself and must be solved self consistently. To find the solution of the OZ eq., we follow the method of Wertheim [12] who used the approximation of Percus and Yevick [15]. The procedure is described as followed:

The PDF is assumed dependent on the temperature, similar to that in the Boltzmann statistics, i.e.  $g(r) = \tau(r)e(r)$ , with  $e(r) = \exp(-\beta u_2(r))$  where  $u_2(r)$  is the potential energy of a pair of particles, and  $\tau(r)$  is a function to be determined. Percus and Yevick have approximated the pair correlation function to the PDF by the equation

$$c(r) = g(r) \left( 1 - \exp \left\{ \frac{u_2(r)}{k_B T} \right\} \right) \tag{7}$$

so that  $c(r) = f(r)\tau(r)$  with  $f(r) = e(r) - 1$ . The OZ eq. in (5) can therefore be written as

$$\tau(r) = 1 - d \int_V f(r') \tau(r') d\vec{r}' + d \int_V e(|\vec{r} - \vec{r}'|) \tau(|\vec{r} - \vec{r}'|) f(r') \tau(r') d\vec{r}' \tag{8}$$

The above equation, known as the Percus-Yevick equation (PY eq.), was used by Wertheim [12] to determine the pair distribution by assuming  $u_2(r)$  as a hard sphere potential. Wertheim has also used the Laplace transform to solve for the result and established an equation of state of the system:

$$\frac{PV}{N k_B T} = \frac{1 + \eta + \eta^2}{(1 - \eta)^3} \tag{9}$$

where  $P$  is the pressure of the system,  $\eta$  the packing fraction, and  $\alpha$  the hard sphere radius. The packing fraction  $\eta$  is defined by the relation  $\eta = \pi d \alpha^3 / 6$ .

The Fourier transform eq. (6) is thus

$$\mathbb{F}[h(r)] = \mathbb{F}[c(r)] + d \mathbb{F} \left[ \int_V c(|\vec{r} - \vec{r}'|) h(r') d\vec{r}' \right] \tag{10}$$

where  $H(k) = \mathbb{F}[h(r)]$  and  $C(k) = \mathbb{F}[c(r)]$ . Hence, the second term of eq. (10) is

$$\begin{aligned} \mathbb{F} \left[ \int_V c(|\vec{r} - \vec{r}'|) h(r') d\vec{r}' \right] &= \frac{1}{(2\pi)^{3/2}} \int_V e^{i\vec{k} \cdot \vec{r}} \int_V c(|\vec{r} - \vec{r}'|) h(r') d\vec{r}' d\vec{r} \\ &= (2\pi)^{3/2} \left[ \frac{1}{(2\pi)^{3/2}} \int_V e^{i\vec{k} \cdot \vec{r}'} h(r') d\vec{r}' \right] \left[ \frac{1}{(2\pi)^{3/2}} \int_V e^{i\vec{k} \cdot (\vec{r} - \vec{r}')} c(|\vec{r} - \vec{r}'|) d\vec{r} \right] \\ &= (2\pi)^{3/2} H(k) C(k) \end{aligned} \tag{11}$$

It should be noted that the Convolution Theorem (see Appendix) has been used to obtain the last integral in eqs. (10) and (11). Hence

$$H(k) = \frac{C(k)}{1 - d(2\pi)^{3/2} C(k)} \quad (12)$$

$$\begin{aligned} C(k) &= \frac{1}{(2\pi)^{3/2}} \int_V e^{i\vec{k}\cdot\vec{r}} c(r) d\vec{r} \\ &= \frac{1}{(2\pi)^{3/2}} 2\pi \int_0^\infty c(r) r^2 \int_{-1}^{+1} e^{ikr\cos\theta} d\cos\theta dr \\ &= \frac{1}{(2\pi)^{1/2}} \int_0^\infty c(r) r \frac{2}{k} \left[ \frac{e^{ikr} - e^{-ikr}}{2i} \right] dr \\ &= \frac{1}{k} \sqrt{\frac{2}{\pi}} \int_0^\infty c(r) r \sin kr dr \end{aligned} \quad (13)$$

In this paper, we use the  $c(r)$  determined by Wertheim in the hard sphere model, namely

$$c(r) = \begin{cases} \lambda_1 + \frac{6\eta\lambda_2 r}{\alpha} + \frac{0.5\eta\lambda_1 r^3}{\alpha^3}, & r \leq \alpha \\ 0, & r > \alpha \end{cases}, \quad (14)$$

where  $\lambda_1 = (1+2\eta)^2/(1-\eta)^4$  and  $\lambda_2 = -(1+0.5\eta)^2/(1-\eta)^4$ .

Substituting  $c(r)$  into eq. (13) gives

$$\begin{aligned} C(k) &= \frac{1}{k} \sqrt{\frac{2}{\pi}} \int_0^\alpha \left[ \lambda_1 r + \frac{6\eta\lambda_2}{\alpha} r^2 + \frac{\eta\lambda_1}{2\alpha^3} r^4 \right] \sin kr dr \\ &= \frac{1}{k} \sqrt{\frac{2}{\pi}} \left[ \int_0^\alpha \lambda_1 r \sin kr dr + \int_0^\alpha \frac{6\eta\lambda_2}{\alpha} r^2 \sin kr dr + \int_0^\alpha \frac{\eta\lambda_1}{2\alpha^3} r^4 \sin kr dr \right] \end{aligned} \quad (15)$$

Results for each above integral are

$$\int_0^\alpha \lambda_1 r \sin kr dr = -\frac{\lambda_1}{k} \alpha \cos k\alpha + \frac{\lambda_1}{k^2} \sin k\alpha \quad (16)$$

$$\int_0^\alpha r^2 \sin kr dr = -\frac{1}{k} \alpha^2 \cos k\alpha + \frac{2}{k^2} \alpha \sin k\alpha + \frac{2}{k^3} \cos k\alpha - \frac{2}{k^3} \quad (17)$$

$$\int_0^\alpha r^4 \sin kr dr = -\frac{\alpha^4}{k} \cos k\alpha + \frac{4\alpha^3}{k^2} \sin k\alpha + \frac{12\alpha^2}{k^3} \cos k\alpha - \frac{24\alpha}{k^4} \sin k\alpha - \frac{24}{k^5} \cos k\alpha + \frac{24}{k^5} \quad (18)$$

Therefore,

$$\begin{aligned} C(k) &= \sqrt{\frac{2}{\pi}} \left[ \alpha \left( -\lambda_1 - 6\eta\lambda_2 - \frac{\eta\lambda_1}{2} \right) \frac{\cos k\alpha}{k^2} + (\lambda_1 + 12\eta\lambda_2 + 2\eta\lambda_1) \frac{\sin k\alpha}{k^3} \right. \\ &\quad \left. + \left( \frac{12\eta\lambda_2 + 6\eta\lambda_1}{\alpha} \right) \frac{\cos k\alpha}{k^4} - \left( \frac{12\eta\lambda_2}{\alpha} \right) \frac{1}{k^4} - \left( \frac{12\eta\lambda_1}{\alpha^2} \right) \frac{\sin k\alpha}{k^5} + \left( \frac{12\eta\lambda_1}{\alpha^3} \right) \frac{(1 - \cos k\alpha)}{k^6} \right] \end{aligned} \quad (19)$$

The simplified form of above equation is

$$\begin{aligned}
C(k) &= \sqrt{\frac{2}{\pi}} \left[ A \frac{\cos k\alpha}{k^2} + B \frac{\sin k\alpha}{k^3} \right. \\
&\quad \left. + C \frac{\cos k\alpha}{k^4} - D \frac{1}{k^4} - E \frac{\sin k\alpha}{k^5} + F \frac{(1 - \cos k\alpha)}{k^6} \right] \\
C(k) &= \sqrt{\frac{2}{\pi}} \left[ A \frac{\cos k\alpha}{k^2} + B \frac{\sin k\alpha}{k^3} + C \frac{\cos k\alpha}{k^4} - D \frac{1}{k^4} - E \frac{\sin k\alpha}{k^5} + F \frac{(1 - \cos k\alpha)}{k^6} \right] \quad (20)
\end{aligned}$$

where

$$\begin{aligned}
A &= \alpha \left( -\lambda_1 - 6\eta\lambda_2 - \frac{\eta\lambda_1}{2} \right), \\
B &= (\lambda_1 + 12\eta\lambda_2 + 2\eta\lambda_1), \\
C &= \left( \frac{12\eta\lambda_2 + 6\eta\lambda_1}{\alpha} \right), \\
D &= \left( \frac{12\eta\lambda_2}{\alpha} \right), \\
E &= \left( \frac{12\eta\lambda_1}{\alpha^2} \right), \\
F &= \left( \frac{12\eta\lambda_1}{\alpha^3} \right).
\end{aligned}$$

The total correlation function  $h(r)$  is therefore the inverse Fourier transform of  $H(k)$ , i.e.

$$h(r) = \mathbb{F}^{-1}[H(k)] = \frac{1}{(2\pi)^{3/2}} \int_V e^{-i\vec{k}\cdot\vec{r}} \frac{C(k)}{1 - (2\pi)^{3/2} d C(k)} d\vec{k} \quad (21)$$

Since  $h(r)$  is spherically symmetric under the isotropic assumption, the integral over the above integral is reduced to

$$h(r) = \frac{1}{r} \sqrt{\frac{2}{\pi}} \int_0^\infty \frac{C(k)}{1 - (2\pi)^{3/2} d C(k)} k \sin kr \, dk \quad (22)$$

Numerical values of  $h(r)$  and  $g(r)$  can be obtained after  $C(k)$  is substituted.

In this paper, the hard sphere parameter  $\alpha$  is not a fixed quantity but assumed to be dependent on the density of the system. Normally, the number density is expressed through a dimensionless radius called  $r_s$ , which is related to the number density  $d$  of the system by the following equation

$$r_s = \left( \frac{3}{4\pi d} \right)^{1/3} \frac{1}{a_0} = \frac{a_1}{a_0} \quad (23)$$



with  $a_0$  representing the Bohr radius and  $a_1$  the volume associated with one atom, i.e.  $4\pi a_1^3/3=1/d$ . Hence  $a_1$ , may also be interpreted as the shortest distance to the next nearest neighbor. In the atomic mass unit, where  $a_0 = 1$ , we have  $r_s = a_1$ .

For  $\alpha = r_s$ , we have the packing fraction  $\eta$  equal to 0.125 which is a very small number compared to the packing fractions of face centered cubic (fcc) and the body-centered cubic (bcc) of solids, namely  $\eta_{fcc} = 0.74$  and  $\eta_{bcc} = 0.68$ . Therefore, if the hard sphere radius is set equal to  $r_s$ , it means that the system has low density. The PDF calculated from this hard sphere radius will be suitable for the system with low density as well. The liquid metallic hydrogen being considering has, of course, high density and does need to get a suitable hard-sphere radius. We employ Wertheim's equation of state in eq. (9) to determine the hard-sphere radii at various pressures. We see from the variation of hard-sphere radii on pressures plotted for  $r_s = 2$  and  $T = 3,000$  K in Fig. 1 that for the pressures in the range of 93-180 GPa the  $\alpha$  is about 3.10 to 3.45 Bohr units or about to 1.6  $r_s$  to 1.7  $r_s$ . The calculated hard sphere radius will be called as the effective hard sphere radius. The experimental physical quantities such as the pressure, the temperature and the density are needed to determine the effective hard sphere radii at different conditions. The  $d, T, P$  from first three rows of Table 1 are obtained from experiments of Weir et al. [1] and our calculated values of the hard sphere radius  $r_s$ , hard sphere parameter  $\alpha$ , and packing fraction  $\eta$  are presented in rows 4-7.

**Table 1** Thermodynamic quantities and the calculated hard sphere radii with corresponding packing fractions. The packing fraction in the last row is approximated to be  $4.41/r_s^3$  since  $\eta = \pi d \alpha^3 / 6$  and the average for the experimental pressure range (93-180 GPa) is 3.28 amu.

$d$ (mole/cm <sup>3</sup> )	0.280	0.289	0.310	0.318	0.327	0.343	0.360
$T$ (Kelvin)	2,200	2,300	2,590	2,780	3,000	3,650	4,400
$P$ (GPa)	93	100	120	130	140	160	180
$r_s(a_0)$	2.123	2.100	2.052	2.035	2.016	1.984	1.952
$\alpha$ (amu)	3.447	3.410	3.331	3.318	3.258	3.177	3.092
$\eta = \pi d \alpha^3 / 6$	0.535	0.535	0.535	0.542	0.528	0.513	0.497
$\eta \cong 4.41/r_s^3$	0.46	0.47	0.51	0.52	0.54	0.56	0.59

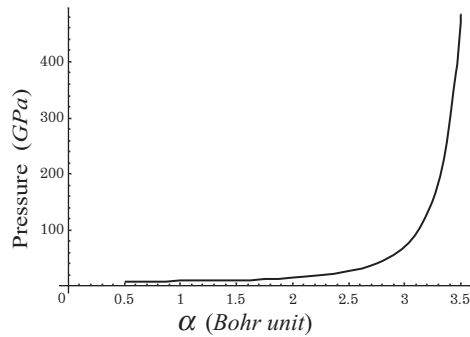


**Figure 1** Variation of hard-sphere radii on pressures plotted for  $r_s = 2$  and  $T = 3,000$  K

The packing fraction in solid structures is well determined because of the fixed positions of ions inside. Packing fractions of well-known Bravais lattices are, for example,  $\eta_{fcc} = 0.74$ ,  $\eta_{bcc} = 0.68$  and  $\eta_{sc} = 0.52$ . We may notice that the packing fraction of the fcc lattice must be the most compact packing. The case of  $\eta > 0.74$  could mean overlapping of atoms (or bases) of the structure. In liquids, the symmetry breaks down and therefore the packing fraction is difficult to obtain. The inter-ion or inter-atomic distance in liquid must be averaged over all possible configurations. Bernal has used random-closed-packed atoms in liquids to get the value of  $\eta = 0.638$ . This value has been accepted to be the maximum possible packing fraction of liquids without assuming overlapping of atomic constituents. Many authors have used  $\eta$  from 0.35 to 0.50 to get values of the PDF and the structure factor  $S(k)$  comparable to the experimental values. However, in the case of liquid metallic hydrogen, there is no experimental value of PDF and  $S(k)$  due to very small mass of atomic hydrogen that make neutron scattering experiment impossible. When the pressure is increased the constituent atoms should be closer and thus the packing fraction should be larger. However, the results in Table 1 provide the decrease of packing fraction due to pressures. The averaged hard-sphere radius in the pressure range of 93 to 180 GPa from the Table is thus  $\bar{\alpha} = 3.28$  amu. We use this averaged value to evaluate the packing fraction via the relation

$$\eta = \frac{1}{6} \pi d \alpha^3 \cong 4.41 / r_s^3 \quad (24)$$

where  $r_s \in [1.952, 2.123]$ .

We therefore can see that the calculated packing fraction increases when the pressure increases. The physical quantities in first three rows in Table 1 are experimental while the rest four rows are calculated ones. Since the temperature effect could expel atoms away from each other and hence increase the packing fraction. In fact, the thermodynamic variables are dependent to each other via the equation of state. However, we assume that the pressure

dominates the temperature effect, and thus the packing fraction should increase. This assumption is reasonably made due to the fact that metallization may occur as the atoms coming closer which certainly increase overlapping of wave functions of electrons in the systems.

## Results

### a) The pair distribution function

We have determined the PDF for three values of  $r_s$  of metallic liquid hydrogen from the basic equation  $g(r) = h(r)-1$  and Wertheim's correlation function

$$h(r) = \frac{1}{r} \sqrt{\frac{2}{\pi}} \int_0^{\infty} \frac{C(k)}{1 - (2\pi)^{3/2} d C(k)} k \sin kr dk \quad (25)$$

and from eq.(20). Comparison of our results with Xu-Hansen's [16] obtained from the density functional theory is shown in Figures 2 to 4. We have also presented in Figure 5 the PDF's at three pressures; 93, 140 and 180 GPa; corresponding to the data shown in Table 2.

**Table 2** The data used in the PDF calculation at three values of  $r_s$ .

$r_s$	0.5	1.0	1.5
$d$ (mole/cm <sup>3</sup> )	21.42	2.68	0.79
$\alpha$ (amu)	0.75	1.54	2.30
$\eta$	0.638	0.638	0.638
$P(\alpha, d)$ (GPa)	4,424	693	197
$P(\eta, d)$ (GPa)	23,000	2,880	782

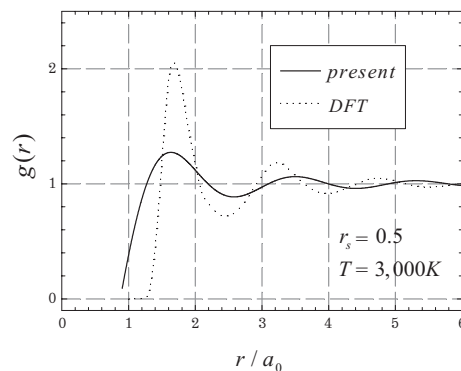


**Figure 2** Calculated PDF's at  $r_s = 0.5$  and  $T = 3,000 K$  compared with that determined using the density functional theory (DFT).

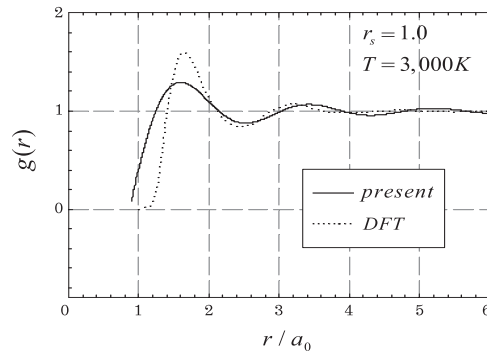


**Figure 3** Calculated PDF's at  $r_s = 1.0$  and  $T = 3,000 K$  compared with that determined using the density functional theory (DFT).

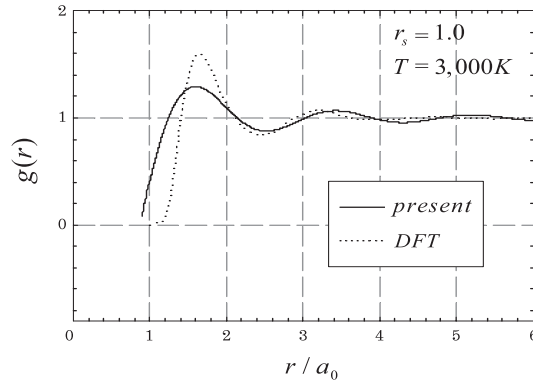


**Figure 4** Calculated PDF's at  $r_s = 1.5$  and  $T = 3,000 K$  and compared with that determined using the density functional theory (DFT).

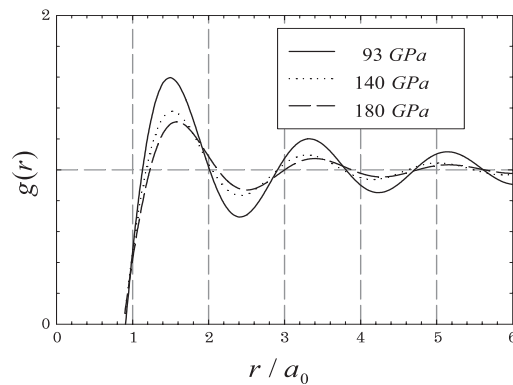


**Figure 5** Comparison of present PDF's at three pressures: 93, 140 and 180 GPa.

In comparison with the DFT results of Xu-Hansen, we can see that the first peaks of our PDF's are very closed to theirs but next peaks shift a bit. The first peak of PDF is the most important since it shows maximum probability of finding the next atom next to the one being considered at the origin. The  $r_s = 0.5, 1.0$  and  $1.5$  correspond to the densities of 21.42, 2.68 and 0.79 mole/ml which is still very far away realistic experiments currently done on earth. Liquid metallic hydrogen achieved experimentally has the density between 0.28 to 0.36 mole/ml. Physicists believe that the very high densities may be available in the core of Jupiter. Calculated PDF's at three pressures are compared and shown in Figure 5. We see that the height of the peak decreases with the increase of the pressure. However, we cannot make any clear conclusion on the pressure since each system has other thermodynamic conditions.

### b) The structure factor

We have determined the structure factor of using the Percus-Yevick equation with the correlation function of Wertheim from the following equation.

$$\begin{aligned}
 S(k) &= 1 + d \int_V \exp(i\vec{k} \cdot \vec{r}) (g(r) - 1) d\vec{r} \\
 &= 1 + d(2\pi)^{3/2} \left[ \frac{1}{(2\pi)^{3/2}} \int_V \exp(i\vec{k} \cdot \vec{r}) h(r) d\vec{r} \right] \\
 &= 1 + d(2\pi)^{3/2} H(k)
 \end{aligned} \tag{26}$$

After substituting  $g(r)$  into eq. (3) we obtain  $S(k)$  in an analytic form as

$$S(k) = \frac{1}{1 - d(2\pi)^{3/2} C(k)}, \tag{27}$$

where  $C(k)$  is the already-determined correlation in momentum space. We may note here that  $S(k)$  is dependent on the transferred momentum  $k$  and the number density  $d$  which is directly related to the effective radius  $\alpha$ . The calculated structure factors at four different pressures are presented in Figures 6-9. The shaded area of the  $S(k)$  shows the values of  $k$  below  $2k_F$ .

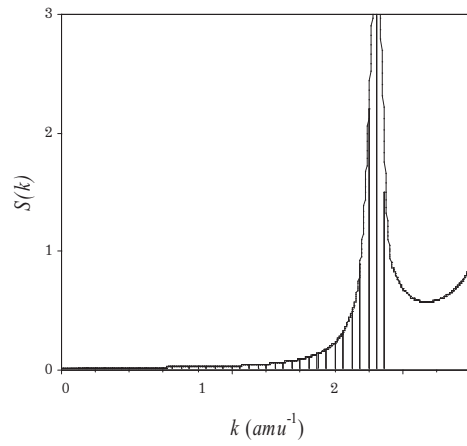


**Figure 6**  $S(k)$  at the pressure of 130 GPa.

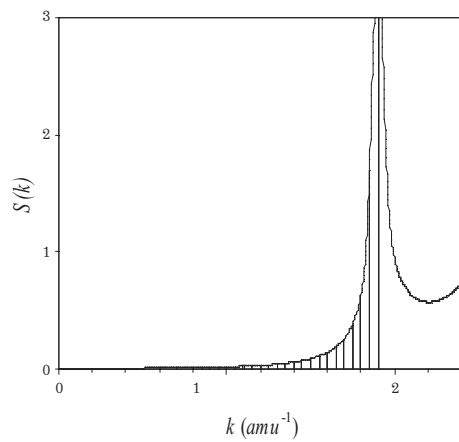


**Figure 7**  $S(k)$  at the pressure of 140 GPa.

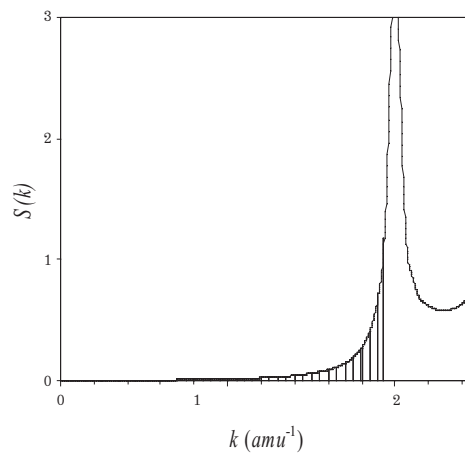


**Figure 8**  $S(k)$  at the pressure of 160 GPa.

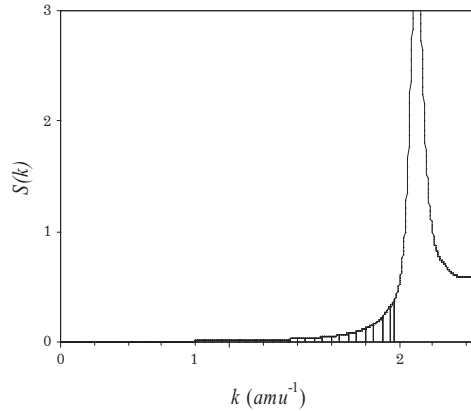


**Figure 9**  $S(k)$  at the pressure of 180 GPa.

### c) The electrical resistivity

Basically, the electrons in our system is assumed to move freely without self scattering, also called plasma scattering, the electrical resistivity of our system is determined using the electrical conductivity formula from the Drude model, namely

$$\rho = \frac{m v_F}{n e^2 \Lambda}, \quad (28)$$

where  $\Lambda = \frac{2\sqrt{2}}{3\pi \varepsilon_F^{1/2}} \frac{\varepsilon_F^2}{\langle S \rangle |U_k|^2}$  is the Fermi velocity with Fermi wave vector determined from the relation with the electron density:  $k_F = (3\pi^2 n)^{1/3}$ . The mean free path  $\Lambda$  is obtained using Ziman's method [17] and the Born approximation, i.e.

$$\frac{1}{\Lambda} = \frac{N_i}{V} 2\pi \int_0^{2\pi} (1 - \cos \theta) \xi(\theta) \sin \theta d\theta \quad (29)$$

where  $N_i$  is the density of scattering centers in the system with scattering differential cross section  $\xi(\theta)$ . Ziman has determined this quantity for spherical symmetric scattering potential to be

$$\xi(\theta) = \frac{2\pi}{\hbar v_F} \left| \frac{1}{N_i} U_k \right|^2 \frac{3}{4} \frac{n}{\varepsilon_F} \frac{1}{4\pi}, \quad (30)$$

where  $U_k$  is the pseudo-potential in momentum space. Ziman has introduced the averaged scattering factor  $\langle S \rangle$  to be

$$\langle S \rangle |U_k|^2 = \frac{1}{4k_F^4} \int_0^{2k_F} |U_k|^2 S(k) k^3 dk . \tag{31}$$

Therefore, the mean free path is

$$\Lambda = \frac{2\sqrt{2}}{3\pi \varepsilon_F^{1/2}} \frac{\varepsilon_F^2}{\langle S \rangle |U_k|^2} \tag{32}$$

We see that our electrons can “see” only ions in the system by neglecting contribution from other electrons. Hence, we [18] use the pseudo-potential introduced by Faber [21] to get

$$U(k) = \frac{4\pi e^2 \lambda^2}{1 + \lambda^2 k^2}, \tag{33}$$

with  $\lambda^2 = \frac{\pi \hbar^2 k_F^2}{3nme^2}$ . We are now able to use eq. (28) with the help of eqs. (32) and (33) to determine the electrical resistivity of the system. Our calculated results at various pressures are compared with the experimental results of Weir et al. [1] in Fig. 10. Details of the results are also presented in Table 3 below.

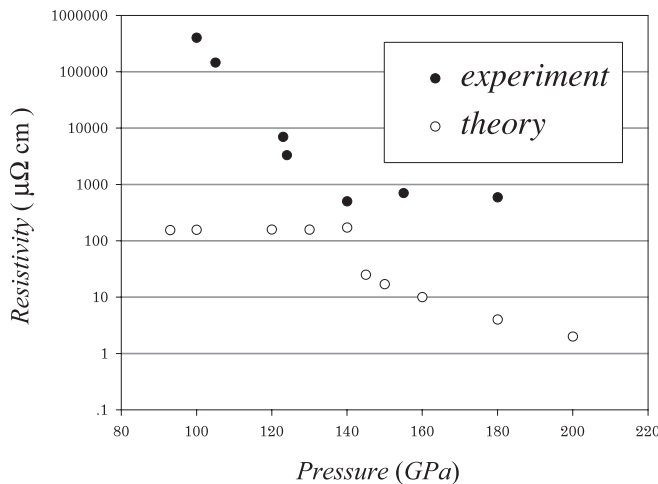


**Figure 10** Calculated resistivity compared with experimental results of Weir et al.



**Table 3** Show the position of the 1<sup>st</sup> peak, the value of  $2k_F$ , and the calculated resistivity at different pressures.

<i>P</i> (GPa)	93	100	120	130	140	160	180
1 <sup>st</sup> peak (amu <sup>-1</sup> )	1.63	1.68	1.79	1.83	1.90	1.98	2.11
<i>k</i> (amu <sup>-1</sup> )	1.81	1.83	1.87	1.89	1.90	1.93	1.97
$\rho$ ( $\Omega$ -cm)	113	104	86	80	47	10	4

## Discussion and Conclusion

The calculated results of pair distribution functions and structure factors of liquid metallic hydrogen using the classical hard sphere potential are presented in the last section. The PDF's have been compared with that calculated from the density functional theory of Xu and Hansen. The first peaks appear to be lower but do not show very much different in position. The calculated PDF's seem to oscillate the same way as that from the DFT theory. In Figure 5, the calculated PDF's at different pressures do not show significant difference in position of the first peak. They just show clearly lower first-peak height at higher pressure. Corresponding structure factors at those pressures are also presented and show a little shift of the first peak in *k* space. Since the experimental result of the PDF's is still not available to compare our results with. The calculated results might not be exact, however they show dependency on physical parameters used. The results are also very much dependent on the classic hard sphere model that seems to be possible to lead to analytical calculation and numerical graphing. However, it is too far and too difficult to interpret this calculation results in terms of what really happen to the liquid such as it is a molecular or atomic liquid, or mixed form. Our next task is to replace the hard sphere model with a more realistic potential such as the collapsing hard sphere model [20, 21] that introduces a small collapsing region of the collision as another parameter. The self-consistent Ornstein-Zernike of this system with the Percus-Yevick approximation should be solved analytically using a mathematical transformation such as the Laplace transform. We conclude from the results that the metal-insulator transition of the metallic hydrogen is speculated to occur when the first peak of the structure factor shifts across  $2k_F$ .

## Appendix: The Convolution Theorem

The Fourier transforms of  $p(y)$  and  $q(y)$  are defined as

$$P(k) = \frac{1}{\sqrt{2\pi}} \int_{-\infty}^{\infty} p(y) e^{iky} dy \quad \text{and} \quad Q(k) = \frac{1}{\sqrt{2\pi}} \int_{-\infty}^{\infty} q(y) e^{iky} dy$$

The Convolution Theorem states that

$$\int_{-\infty}^{\infty} p(y) q(x-y) dy = \int_{-\infty}^{\infty} P(k) Q(k) e^{-ikx} dk$$

This can be proved as following

$$\begin{aligned} \int_{-\infty}^{\infty} p(y) q(x-y) dy &= \frac{1}{\sqrt{2\pi}} \int_{-\infty}^{\infty} p(y) \int_{-\infty}^{\infty} Q(k) e^{-ik(x-y)} dk dy \\ &= \frac{1}{\sqrt{2\pi}} \int_{-\infty}^{\infty} Q(k) \left[ \int_{-\infty}^{\infty} p(y) e^{iky} dy \right] e^{-ikx} dk \\ &= \int_{-\infty}^{\infty} Q(k) P(k) e^{-ikx} dk \end{aligned}$$

and from 
$$\int_{-\infty}^{\infty} p(y) q(x-y) dy = \frac{1}{\sqrt{2\pi}} \int_{-\infty}^{\infty} p(y) \int_{-\infty}^{\infty} Q(k) e^{-ik(x-y)} dk dy$$

by defining the new variable  $z = x-y$  so that  $y = x-z$  and  $dy = -dz$ . Substituting  $y$  and  $dy$  into above equation leads to

$$\begin{aligned} \int_{-\infty}^{\infty} p(x-z) q(z) dz &= \frac{1}{\sqrt{2\pi}} \int_{-\infty}^{\infty} p(x-z) \left[ \int_{-\infty}^{\infty} Q(k) e^{-ikz} dk \right] dz \\ &= \frac{1}{\sqrt{2\pi}} \int_{-\infty}^{\infty} Q(k) \int_{-\infty}^{\infty} p(x-z) e^{ik(x-z)} dz e^{-ikx} dk \\ &= \int_{-\infty}^{\infty} Q(k) P(k) e^{-ikx} dk \end{aligned}$$

Hence 
$$\int_{-\infty}^{\infty} p(x-z) q(z) dz = \int_{-\infty}^{\infty} P(k) Q(k) e^{-ikx} dk,$$

and therefore 
$$\int_{-\infty}^{\infty} p(y) q(x-y) dy = \int_{-\infty}^{\infty} p(x-y) q(y) dy$$

## References

1. Weir, S. T., Mitchell, A. C., and Nellis, W. J. 1996. Metallization of Fluid Molecular Hydrogen at 140 GPa (1.4 Mbar). *Physical Review Letters* 76: 1860-1863.
2. Wigner, E., and Huntington, H. B. 1935. On the Possibility of a Metallic Modification of Hydrogen. *Journal of Chemical Physics* 3: 764-770.
3. Bastea, M., Mitchell, A. C., and Nellis W. J. 2001. High Pressure Insulator-Metal Transition in Molecular Fluid Oxygen. *Physical Review Letters* 86: 3108-3111.
4. Shvets, V. T., Savenko, S. V., and Malynovski, Y. K. 2006. Ionic Interaction and Conductivity of Metallic Hydrogen. *Condensed Matter Physics* 9: 127-133.
5. Shvets, V. T. 2007. High Temperature Equation of State of Metallic Hydrogen. *Journal of Experimental and Theoretical Physics* 104: 655-660.
6. Shvets, V. T. 2008. Electrical Conductivity of Metallic Hydrogen as a Ternary System. *High Temperature* 46: 219-224.
7. Ceperley, D. M., and Alder, B. J. 1987. Ground State of Solid Hydrogen at High Pressures. *Physical Review* B36: 2092-2106.
8. Barbee, T. W., Garcia, A., Cohen, M. L., and Martins, J. L. 1989. Theory of High-Pressure Phases of Hydrogen. *Physical Review Letters* 62: 1150-1153.
9. Holmes, N. C., Ross, M., and Nellis, W. J. 1995. Temperature Measurements and Dissociation of Shock-Compressed Liquid Deuterium and Hydrogen. *Physical Review* B52: 15835-15845.
10. Kohanoff, J., and Hansen, J. P. 1996. Statistical Properties of Dense Hydrogen Plasma: An ab initio Molecular Dynamics Investigation. *Physical Review* E54: 768.
11. Ceperley, D. M. 1992. Path-Integral Calculations of Normal Liquid  $^3\text{He}$ . *Physical Review Letters* 69: 331-334.
12. Wertheim, M. S. 1963. Exact Solution of the Percus-Yevick Integral Equation for Hard Spheres. *Physical Review Letters* 10: 321-323
13. Wertheim, M. S. 1964. Analytic Solution of the Percus-Yevick Equation. *Journal of Mathematical Physics* 5: 643-651.
14. Percus, J. K., and Yevick, G. J. 1958. Analysis of Classical Statistical Mechanics by Means of Collective Coordinates. *Physical Review* 110: 1-13.
15. Bernal, J. D. 1960. Geometry of the Structure of Monatomic Liquids. *Nature (London)* 185: 68-70.
16. Xu, H., and Hansen, J. P. 1998. Density Functional Theory of Pair Correlations in Metallic Hydrogen. *Physical Review* E57: 211-223.

17. Ziman, J. M. 1961. A Theory of Electrical Properties of Liquid Metals I. The Monovalent Metals. *Philosophical Magazine* 6: 1013-1034.
18. Konjanatnikorn, R. 2001. Pair Distribution Function in Liquid Hydrogen. Master Degree Thesis. Bangkok. Chulalongkorn University.
19. Faber, T. E. 1973. IAEA-SMR-46/125; An Introduction to the Theory of Liquid Metals. Cambridge. Cambridge University Press. p 645.
20. Ryzhov, V. N., and Stishov, S. M. 2002: A Liquid-Liquid Phase Transition in the Collapsing Hard Sphere System. *Journal of Experimental and Theoretical Physics* 95: 710-713.
21. Stishov, S. M. 2002. On Phase Diagram of the System of Collapsing Hard Spheres. *Journal of Experimental and Theoretical Physics* 95: 64-66.

ได้รับบทความวันที่ 3 พฤษภาคม 2554  
ยอมรับตีพิมพ์วันที่ 28 มิถุนายน 2554